*Biomineralization*

DOI: 10.1002/ange.200501654

# Self-Organizing β-Sheet Lipopeptide Monolayers as Template for the Mineralization of $CaCO_3$**

*Silvia Cavalli, Daniela C. Popescu, Emily E. Tellers, Matthijn R. J. Vos, Benoît P. Pichon, Mark Overhand, Hanna Rapaport, Nico A. J. M. Sommerdijk,* and Alexander Kros**

The large variation in inorganic structures encountered in biological systems, often with exquisite and unique morphologies, has fascinated researchers in all scientific disciplines for a long time.[1] For materials scientists, an understanding of the principles underlying the process of biomineralization holds great promise for the design and synthesis of new inorganic and hybrid structures with yet unrealized properties. The central concept in biomineralization research is that organized biomacromolecules, which contain well-defined arrays of functional groups, control polymorph selection and the oriented nucleation of crystals by lowering the nucleation energy of specific crystal faces.[2] Control over crystal morphology is then exerted by the interaction of biomolecules in solution with specific crystal planes during growth.

Recently, it has become clear that the classical concept, which proposes that a template containing well-defined arrays of functional groups controls the nucleation of the inorganic crystals by geometric and stereochemical matching, needs expanding.[3] Furthermore, a crucial role for amorphous calcium carbonate as a transient intermediate has been proposed.[4] In the last few years it was demonstrated that specific nucleation of calcite can be achieved without an

[*] D. C. Popescu,[+] M. R. J. Vos, Dr. B. P. Pichon, Dr. N. A. J. M. Sommerdijk
Laboratory of Macromolecular and Organic Chemistry
Eindhoven University of Technology
P.O. Box 513, 5600 MB, Eindhoven (The Netherlands)
Fax: (+31) 40-245-1036
E-mail: n.sommerdijk@tue.nl

S. Cavalli,[+] E. E. Tellers, Dr. M. Overhand, Dr. A. Kros
Leiden Institute of Chemistry, Leiden University
P.O. Box 9502, 2300 RA, Leiden (The Netherlands)
Fax: (+31) 71-527-4397
E-mail: a.kros@chem.leidenuniv.nl

Dr. H. Rapaport
Department of Biotechnology Engineering
Ben Gurion University of the Negev
P.O. Box 653, 84105 Beer-Sheva (Israel)

[+] These authors contributed equally.

[**] We are grateful to Wim Jesse, Hans van den Elst, and Nico Meeuwenoord for their technical assistance. Hugo Simões and Jan-Willem Handgraaf are acknowledged for the graphics. We thank Dr. J. Aizenberg for fruitful discussions. This research was supported by the Netherlands Scientific Organization (NWO) through an open competition grant (D.C.P.) and a VENI grant (A.K.).

Supporting information for this article is available on the WWW under http://www.angewandte.org or from the author.

epitaxial match with the exposed crystal planes,[5–7] and it has been suggested that electrostatic interactions play an important role in the control of the orientation of crystal growth.[8,9]

In nature crystal nucleation and growth are often controlled by carboxylate-rich polypeptides (containing, for example, aspartate and glutamate), which are present within a macromolecular matrix with organized β-sheet domains.[10] Although (poly)peptides have been successfully employed as additives that are capable of modifying the growth of calcium carbonate crystals,[11] there have been few reports in which peptides with predefined secondary structures have been studied as templates for mineralization.[9a,12–14] Recently, it was demonstrated that amphiphilic peptides comprising phenylalanine (Phe) and glutamic acid (Glu) residues can form ordered Langmuir monolayers with a β-pleated sheet structure at the air/water interface.[15]

We have modified the water-soluble $(Leu\text{-}Glu)_4$ octapeptide motif **1** with a phospholipid moiety (dioleoyl phosphatidyl ethanolamine, DOPE) to increase its amphiphilicity so that it would form stable monolayers at the air/water interface. We anticipated that the resulting lipopeptide **2** should be able to form a β-sheet structure, thereby exposing an ordered array of carboxylate groups to the aqueous phase. Herein, we report how this monolayer interacts with $Ca^{2+}$ ions and is employed subsequently as a biomimetic mineralization template for the formation of a new crystal habit of calcite.

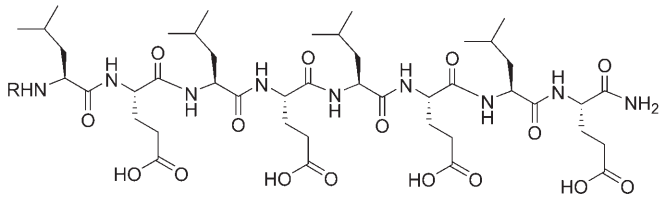

**1**: R = H
**3**: R = C(O)CH$_3$

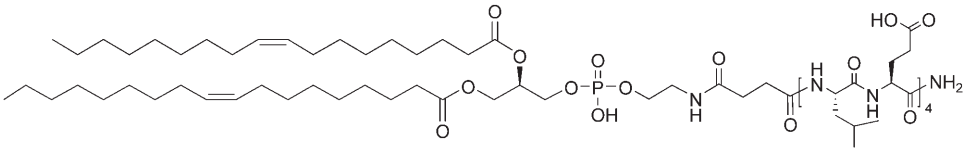

**2**

Surface-pressure–surface-area (π–A) isotherms of the resulting lipopeptide **2** were characterized by an apparent condensed liquid phase that was present over a rather large trajectory (Figure 1a). The slope of the isotherm indicated a fluidlike character of the monolayer, most probably provided by the unsaturated lipid chains.[16] Brewster angle microscopy (BAM) images (not shown) revealed that **2** self-assembled into preformed domains with millimeter dimensions. These domains, which were present in the expanded state, fused upon compression to form a continuous film. The compressed monolayer was transferred to quartz plates and ZnSe prisms for CD and FTIR analysis, respectively (see the Supporting Information for details). The β-sheet structure was confirmed by the appearance of a CD signal displaying a maximum at 202 nm and a minimum at 218 nm,[17] as well as by an amide I vibration at 1628 $cm^{-1}$ in the FTIR spectrum. The small IR band at 1694 $cm^{-1}$ indicated an antiparallel organization of the strands (Figure 1c,d).[18] The β-sheet organization of lipopeptide **2** at the air/water interface was further confirmed by in situ grazing incidence X-ray diffraction (GIXD) measurements (see the Supporting Information).[19]

To verify the stability of the lipopeptide secondary structure upon complexation with $Ca^{2+}$ ions, isotherms were recorded with an aqueous $CaCl_2$ solution (10 mM) as the subphase (Figure 1a). An expansion in molecular area from 189 to 202 $Å^2$ molecule$^{-1}$ was observed; however, the CD and IR spectra of the transferred monolayers still revealed the spectroscopic characteristics typical of β-pleated strands (see the Supporting Information). A further expansion of the molecular area to approximately 250 $Å^2$ molecule$^{-1}$ was observed when **2** was spread on a subphase containing $Ca(HCO_3)_2$ (9 mM, Figure 1a), which is the solution used in the crystallization experiments described below.[20] In this case BAM no longer revealed the formation of domains, either before or upon compression. These results indicate that, on account of the DOPE moiety, the lipopeptide **2** forms a monolayer that self-assembles without compression, but is still dynamic and adapts its structure upon complexation of calcium ions to interact efficiently with the nucleating crystals.

Calcium carbonate crystals were grown under self-organized monolayers of **2** ($\pi = 30\ mN\,m^{-1}$) by using the Kitano method[20] and collected after 5, 20, and 48 h. Calcite was produced predominantly in the form of pyramidal crystals together with rhombohedral crystals having a concave central region.[21] The pyramidal crystals were characterized by three thermodynamically stable {10.4} faces that were oriented to the aqueous phase and one face consisting of three facets that was oriented to the monolayer (Figure 2a). Crystals with a similar elevated feature consisting of three inclined facets have been observed before.[6b,9c,22] It was suggested that the apex represented the initial point of attachment to the monolayer, and that the outer edges of the crystal detached in time from the monolayer as a result of gravity. Computer modeling of the crystals based on scanning electron micrographs[23] indicated that, in almost all cases, the facetted faces belonged to the class {01.*l*}, with *l* ranging from 1–2. The formation of this class of crystal faces in solution has been reported frequently for biogenic calcite,[24] and recently also for the octapeptide $(Phe\text{-}Asp)_4$.[9a] In addition, (01.2)-oriented calcite crystals were obtained with different monolayer systems.[5,6a,9b,25,26]

Previously, Lahiri et al. reported the formation of calcite crystals with symmetrical indentation defined by three {01.2} faces around a (00.1) face, which formed the attachment point to a porphyrin monolayer.[27] In the present case the concave indentation of these crystals is defined by four roughened

  

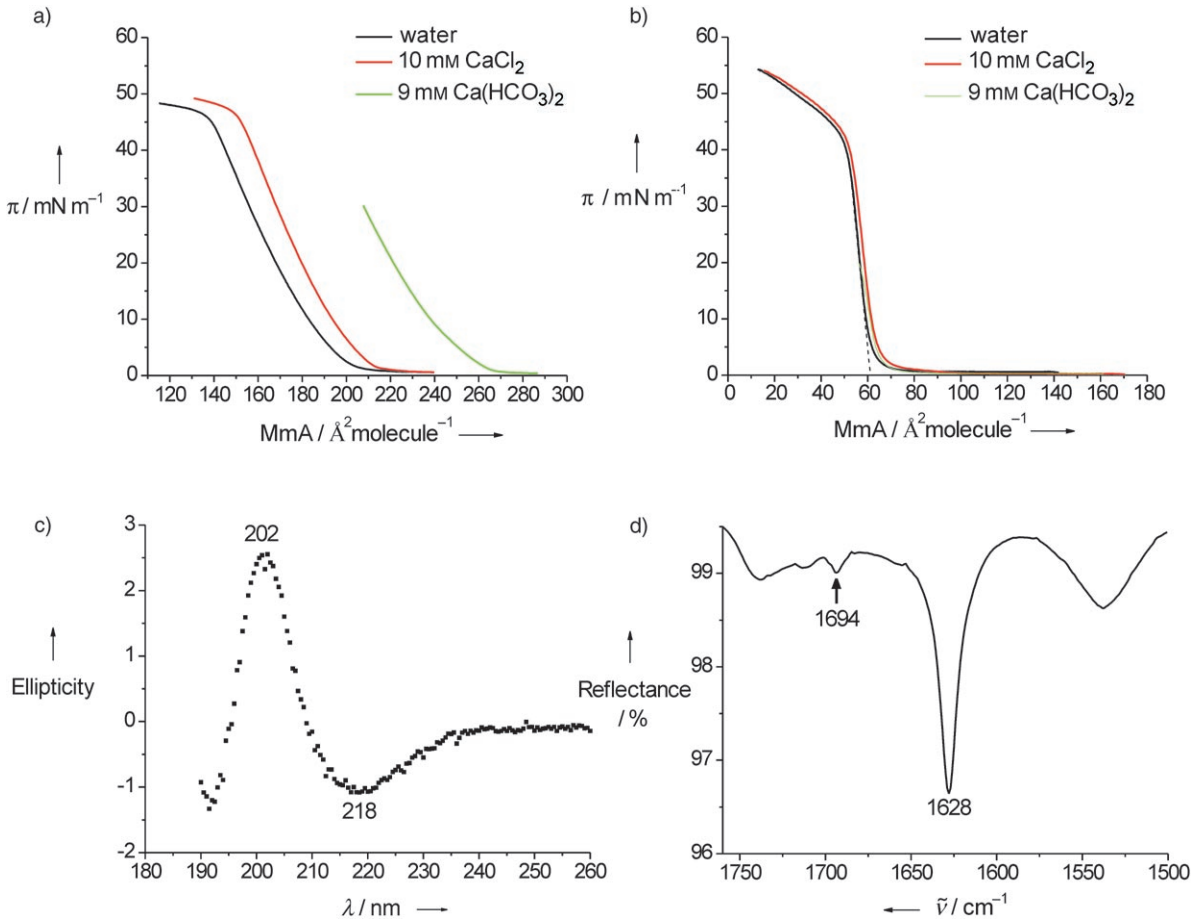


***Figure 1.*** π–A isotherms of the monolayer of a) lipopeptide **2** and b) N-acetylated octapeptide **3** on (——) $H_2O$, (——) $CaCl_2$ (10 mM), and (——) $Ca(HCO_3)_2$ (9 mM) subphases at 20 °C. The limiting molecular areas for compounds **2** and **3** were determined by extrapolating the slope in the liquid condensed region to zero pressure (see dashed line as an example for **3**).[15] c) CD and d) FTIR spectra of the monolayer of lipopeptide **2** transferred from a water subphase at $\pi = 30\ mN\,m^{-1}$ at 20 °C.

planes (Figure 2b), the outer edges of which form a plane that can be modeled by the $(1\bar{1}.\bar{4})$ face of calcite. However, this morphological appearance of indented rhombohedral crystals has not, to our knowledge, been reported before. Also in the present case, a central patch could be located on several crystals (Figure 2c). The indented crystals were dominant over the pyramidal crystals after 5, 20, and 48 h and this population slightly increased with time (Figure 3a). Selected-area electron diffraction performed on crystals with a rhombohedral shape collected within 20 minutes after the start of the experiment revealed that these crystals had a {10.0} orientation (Figure 2c). This finding suggests that for the indented crystals, crystal nucleation starts from a {10.0} face.

Crystal indentation might be the combined result of gravity and limited $Ca^{2+}$ and $HCO_3^{2-}$ ion transport from the mineralization solution. As the crystal grows it becomes heavier and tends to sink, while still being attached to the monolayer. Being flexible, the monolayer presumably bends to follow the sinking crystal. This will create a gap between the monolayer and the face of the crystal attached to it, toward the edges of the crystal (Figure 3c). Therefore, the hindering effect of the monolayer on ion transport will also be reduced in that region. This allows the outer corners of the crystal facing the monolayer to grow upwards, thus creating an indentation in the crystal.

The N-acetylated octapeptide **3** was also prepared for comparison. The π–A isotherm of **3** revealed a sharp transition from the gaseous to the solid phase (Figure 1b). A molecular area of 61 $Å^2$molecule$^{-1}$ was determined from this curve, a value which was lower than expected (130 $Å^2$molecule$^{-1}$ [28]), probably as a result of the high water solubility of **3**. CD and FTIR studies of the transferred monolayers indicated the presence of an antiparallel β-sheet structure (see the Supporting Information). The CD spectrum displayed a maximum at 201 nm and a minimum at 221 nm, while the IR spectra showed a strong band at 1627 $cm^{-1}$ and a weak one at 1694 $cm^{-1}$.[29] When the isotherm of **3** was recorded on a $CaCl_2$ subphase (10 mM) or on a subphase containing $Ca(HCO_3)_2$ (9 mM) no expansion of the monolayer was observed, which suggests that **3**, in contrast to lipopeptide **2**, does not significantly adapt its structure upon exposure to $Ca^{2+}$ ions (Figure 1b).

Crystals grown under monolayers of **3** again showed both types of modifications. However, in this case predominantly pyramidal crystals were observed after five hours and only a minor (< 5 %) amount of indented crystals was present. The latter population increased to approximately 50 % of the total

  

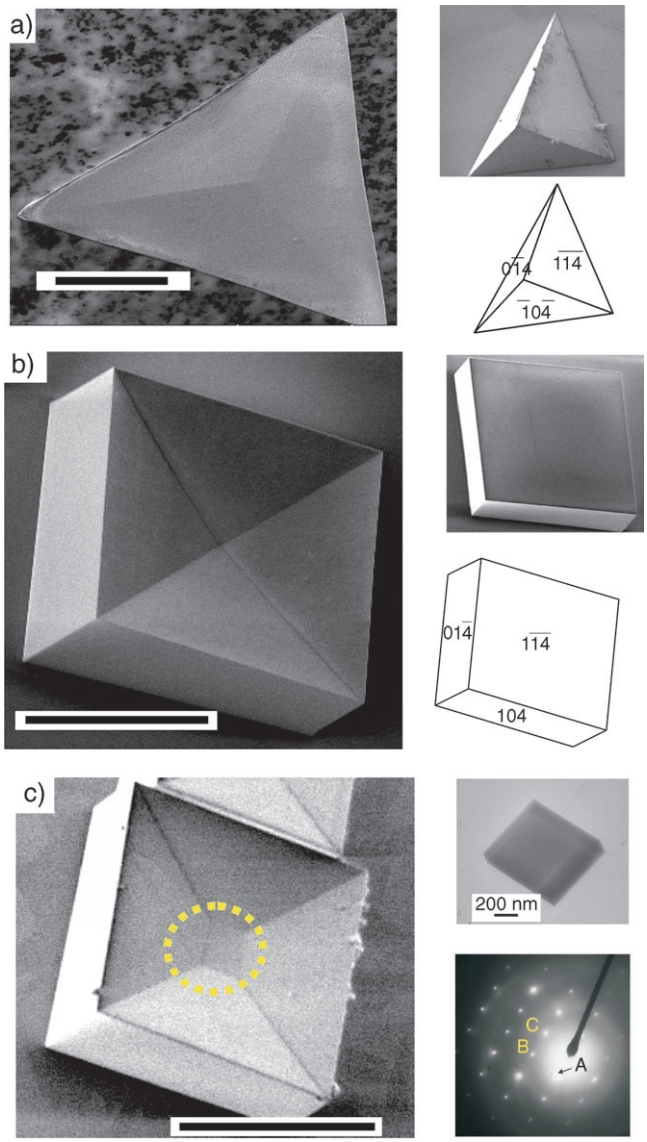


***Figure 2.*** Calcite crystals grown under monolayers of **2**. a) Left: SEM image of a (01.2)-oriented pyramidal crystal as observed from the side attached to the monolayer; right: model[23] and SEM image of a similar crystal viewed from the side exposed to the solution. b) Left: SEM image of a rhombohedral crystal with a concave central region from the side attached to the monolayer; right: model and SEM image of a similar crystal viewed from the side exposed to the solution. c) Left: SEM image of an indented crystal showing a central patch; right: TEM image and electron diffraction pattern of a rhombohedral crystal isolated after 20 min. The pattern corresponds to the [10.0] zone of calcite. Reflections A $(0\bar{1}.\bar{1})$ 4.2 Å; B $(0\bar{1}.4)$ 3.0 Å; C (00.5) 3.4 Å. Angles $(0\bar{1}.\bar{1})\wedge(00.5) = 104°$; $(0\bar{1}.\bar{1})\wedge(0\bar{1}.4) = 59°$. Camera length = 60 cm. Bars represent 20 μm except when indicated otherwise.

number of modified crystals after 20 hours, and only became predominant after 48 hours (65%, Figure 3b). Importantly, most of the pyramidal crystals increased in size rather than in number, which suggests that their nucleation only occurred in the earlier stages of the experiment. In contrast, we observed the appearance of small indented crystals throughout the whole experiment, thus indicating that these crystals also nucleated in the later stages of the experiment.

From the change of the composition of the mineral phase with time, it is apparent that the monolayers of **2** and **3** differ in their ability to nucleate the indented versus pyramidal morphology at the different time points. We propose that in the case of **3**, the nucleation of the face leading to the indented calcite takes place in the later stages of the experiments, probably because the solidlike monolayer needs more time to reorganize and to adapt to the growing crystals.

The {01.1} and {01.2} crystal planes are defined by the same 4.99 Å distance in one direction, but show a gradual change in the orientation of the carbonate groups which are rotated over approximately 10° on going from $l = 1$ to $l = 2$ (Figure 4). The 4.99 Å distance most probably relates to the interstrand distance in the template as defined by the hydrogen bonds in the β-sheet (4.7–4.8 Å; GIXD, see the Supporting Information), which allows an approximate match of the template carboxylate groups with the carbonate ions in the crystal plane. Although there is only a 10° rotation between the planes with $l = 1$ and $l = 2$, significant differences are found in the interion distances in the different nucleation planes. It is therefore likely that in this direction the alignment of the carboxylate groups with respect to the carbonate ions plays a much more important role than the matching of the distances of the two phases.

The more adaptable monolayer of **2** clearly favors the formation of a different set of planes, that is, those belonging to the {10.0} family. Interestingly, these planes are related to the {01.*l*} planes ($l = 1$ or 2) by a further rotation of the carbonate ions (Figure 4). The {10.0} faces are again defined by a distance of 4.99 Å in one direction and have a spacing of 8.53 Å in the other direction. These data suggest that in this case the spacing of 4.99 Å also relates to the interstrand distance of 4.7–4.8 Å in the β-sheet. The interaction of the carboxylate groups of the template with the {10.0} faces along the other direction is most likely related to the ability of the monolayer to adapt to the growing crystal.

The surface-pressure–surface-area isotherms recorded on $H_2O$ and $Ca(HCO_3)_2$ subphases showed an expansion of the mean molecular area from 189 to 250 $Å^2$ molecule$^{-1}$, respectively. We presume that the expansion in the direction of the backbone of the molecule should account for most of the observed increase in mean molecular area.[30] If a small expansion in the interstrand distance from 4.7–4.8 to 4.99 Å is envisioned, the molecule should then expand from ≈40 to ≈50 Å (that is, by about 25%) along its long axis. It is important to note, however, that stretching of the peptide backbone alone to an all-*trans* configuration yields a maximum distance between the Glu side chains of about 7.6 Å compared to the 8.53-Å spacing of the {10.0} face. Nevertheless, the flexibility of the template should allow it to organize such that the carboxylate groups align with the carbonate ions in the nucleation plane while matching the 4.99 Å distance, similar to the proposal for amide-containing phospholipid derivatives.[6] However, other factors, such as the charge density of the amphiphile and the possible presence of a layer of carbonate ions between the crystal and the monolayer, should not be neglected.[8c,9] We propose that the N-acetylated octapeptide **3** has a limited ability to

  

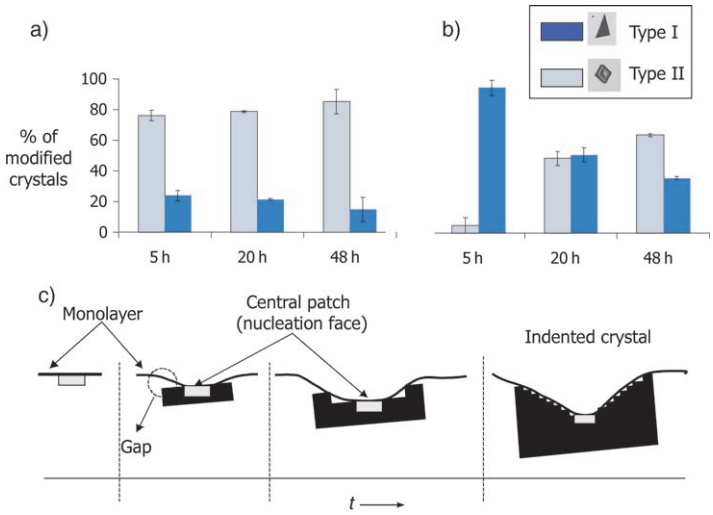


***Figure 3.*** Distribution of the two populations of crystals (Type I: pyramidal shape; Type II: indented crystals) nucleated under monolayers of a) lipopeptide **2** and b) N-acetylated octapeptide **3**, as a percentage of the number of modified crystals (crystals isolated after 5, 20, and 48 h). c) Proposed model for the formation of indented crystals.

adapt to the growing crystal, and hence is responsible for the preferred nucleation of the {01.*l*} faces ($l=1$ or 2) and the much slower formation of the indented crystals.

In conclusion, we have demonstrated that amphiphilic lipopeptide **2** forms stable monolayers with an antiparallel β-sheet conformation. This finding enabled us not only to study the effect of these monolayers on the crystallization of calcium carbonate, but also to investigate interactions with the developing mineral phase. Indeed, the formation of habit-modified calcite was observed. Apart from a small amount of pyramidal {01.*l*}-oriented crystals ($l=1$ or 2), the majority of the modifications resulted in a new type of indented calcite crystal, which according to electron diffraction studies nucleated from a {10.0} face. The formation of this morphological form was significantly suppressed when the less adaptable peptide **3** was used.

In previous studies, the formation of crystals with the {01.2}[6a,25,26] and {10.0}[6b,31] orientations was related to geometrical lattice matching and stereochemical complementarity between the functional groups of the template and the positions of ions in the nucleation plane. In other studies, the oriented nucleation of crystals was attributed to nonspecific electrostatic effects rather than to an epitaxial match between the monolayer and the crystal face.[8,9] We have demonstrated that the nucleation of different crystal faces can be achieved depending on the ability of the template to adapt to the structure of the inorganic phase. Although the importance of the flexibility of the template has been known for many years,[32] it is rarely taken into account in reports on crystal nucleation. Furthermore, the results indicate that stretching of the template in only one direction allows the reorientation of its functional groups, so that the

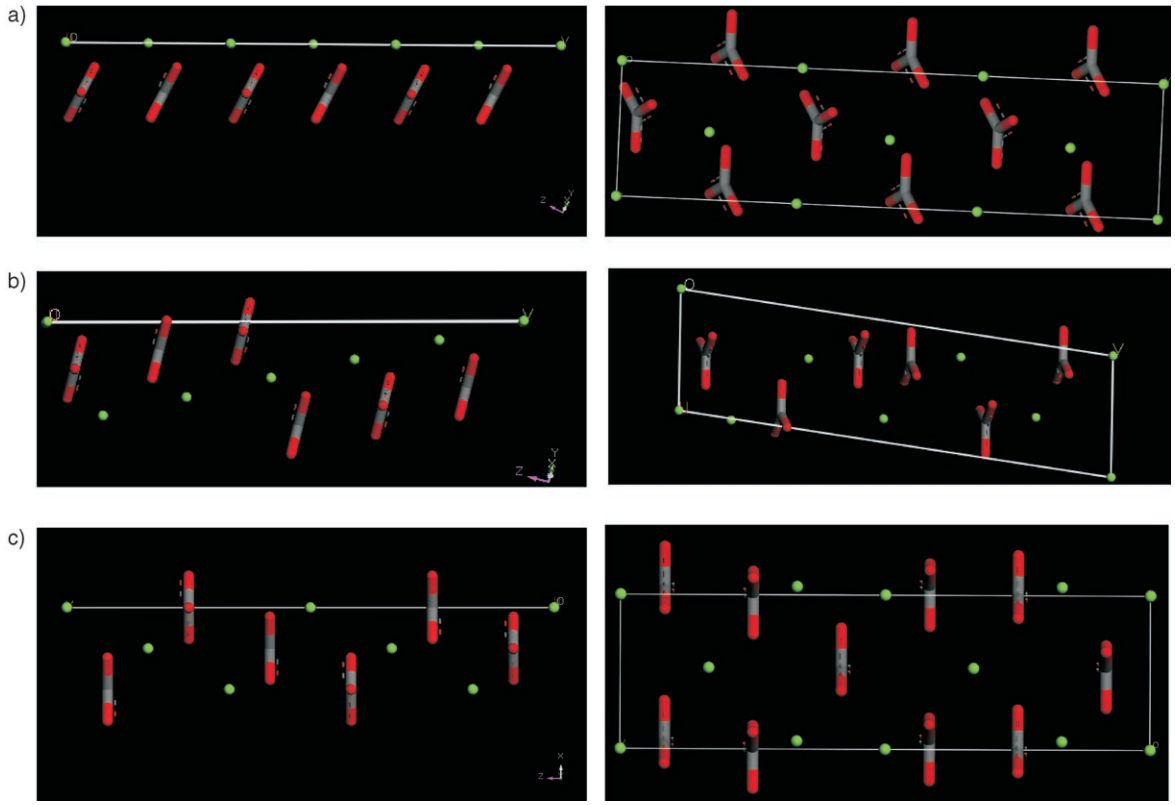


***Figure 4.*** Models of the a) (01.2), b) (01.1), and c) (10.0) planes of calcite with the viewing direction along (left) and perpendicular to (right) the plane.

stabilization of different crystal planes can be achieved without the need for an epitaxial relation between the two components.

Received: May 13, 2005
Revised: August 17, 2005
Published online: October 18, 2005

**Keywords:** calcium · crystal growth · lipopeptides · monolayers · template synthesis

[1] P. Q. Harting, *Q. J. Microsc. Sci.* **1872**, *12*, 118 – 123.
[2] S. Mann, *Nature* **1988**, *332*, 119 – 124.
[3] H. Cölfen, S. Mann, *Angew. Chem.* **2003**, *115*, 2452 – 2468; *Angew. Chem. Int. Ed.* **2003**, *42*, 2350 – 2365.
[4] a) Y. Politi, T. Arad, E. Klein, S. Weiner, L. Addadi, *Science* **2004**, *306*, 1161 – 1164; b) L. Addadi, S. Raz, S. Weiner, *Adv. Mater.* **2003**, *15*, 959 – 970.
[5] a) J. Aizenberg, A. J. Black, G. M. Whitesides, *Nature* **1999**, *398*, 495 – 498; b) A. M. Travaille, J. J. J. M. Donners, J. W. Gerritsen, N. A. J. M. Sommerdijk, R. J. M. Nolte, H. van Kempen, *Adv. Mater.* **2002**, *14*, 492 – 495.
[6] a) S. Champ, J. A. Dickinson, P. S. Fallon, B. R. Heywood, M. Mascal, *Angew. Chem.* **2000**, *112*, 2828 – 2831; *Angew. Chem. Int. Ed.* **2000**, *39*, 2716 – 2719; b) P. J. J. A. Buijnsters, J. J. J. M. Donners, S. J. Hill, B. R. Heywood, R. J. M. Nolte, B. Zwanenburg, N. A. J. M. Sommerdijk, *Langmuir* **2001**, *17*, 3623 – 3628.
[7] J. J. J. M. Donners, R. J. M. Nolte, N. A. J. M. Sommerdijk, *J. Am. Chem. Soc.* **2003**, *124*, 9700 – 9701.
[8] a) D. M. Duffy, J. H. Harding, *Langmuir* **2004**, *20*, 7630 – 7636; b) D. M. Duffy, J. H. Harding, *Langmuir* **2004**, *20*, 7637 – 7642; c) D. M. Duffy, A. M. Travaille, H. van Kempen, J. H. Harding, *J. Phys. Chem. B* **2005**, *109*, 5713 – 5718.
[9] a) D. Volkmer, M. Fricke, T. Huber, N. Sewald, *Chem. Commun.* **2004**, *16*, 1872 – 1873; b) D. Volkmer, M. Fricke, C. Agena, J. Mattay, *J. Mater. Chem.* **2004**, *14*, 2249 – 2259; c) D. Volkmer, M. Fricke, D. Vollhardt, S. Siegel, *J. Chem. Soc. Dalton Trans.* **2002**, 4547 – 4554.
[10] S. Mann, *Biomineralization: Principles and Concepts in Bioinorganic Materials Chemistry*, Oxford University Press, New York, **2001**.
[11] a) L. Addadi, S. Weiner, *Proc. Natl. Acad. Sci. USA* **1985**, *82*, 4110 – 4114; b) L. A. Gower, D. A. Tirrell, *J. Cryst. Growth* **1998**, *191*, 153 – 160; c) T. Sugawara, Y. Suwa, K. Ohkawa, H. Yamamoto, *Macromol. Rapid Commun.* **2003**, *24*, 847 – 851.
[12] a) L. Addadi, J. Moradian, E. Shay, N. G. Maroudas, S. Weiner, *Proc. Natl. Acad. Sci. USA* **1987**, *84*, 2732 – 2736; b) H. Bekele, J. H. Fendler, J. W. Kelly, *J. Am. Chem. Soc.* **1999**, *121*, 7266 – 7267; c) D. B. DeOliveira, R. A. Laursen, *J. Am. Chem. Soc.* **1997**, *119*, 10627 – 10631; d) G. Falini, S. Fermani, M. Gazzano, A. Ripamonti, *J. Chem. Soc. Dalton Trans.* **2000**, 3983 – 3987; e) J. E. Meegan, A. Aggeli, N. Boden, R. Brydson, A. P. Brown, L. Carrick, A. R. Brough, A. Hussain, R. J. Ansell, *Adv. Funct. Mater.* **2004**, *14*, 31 – 37.
[13] M. Bertrand, A. Brack, *Chem. Eur. J.* **2000**, *6*, 3452 – 3455.
[14] Y. Levi, S. Albeck, A. Brack, S. Weiner, L. Addadi, *Chem. Eur. J.* **1998**, *4*, 389 – 396.
[15] H. Rapaport, K. Kjaer, T. R. Jensen, L. Leiserowitz, D. A. Tirrell, *J. Am. Chem. Soc.* **2000**, *122*, 12523 – 12529.
[16] M. Lindén, J. B. Rosenholm, *Langmuir* **1995**, *11*, 4499 – 4504.
[17] A. Rodger, B. Nordén, *Circular Dichroism and Linear Dichroism*, Oxford University Press, New York, **1997**, p. 21.
[18] M. Jackson, H. H. Mantsch, *Crit. Rev. Biochem. Mol. Biol.* **1995**, *30*, 95 – 120.
[19] Details of the GIXD measurements will be part of a forthcoming publication.
[20] Y. Kitano, K. Park, D. W. Hood, *J. Geophys. Res.* **1963**, *67*, 4873 – 4874.
[21] In the absence of a monolayer only unmodified calcite and some vaterite crystals were isolated.
[22] S. Mann, B. R. Heywood, S. Rajam, J. B. A. Walker, *J. Phys. D* **1991**, *24*, 154 – 164.
[23] Calcite crystals were modeled with SHAPE V7.1.2., Shape Software, Kingsport, USA, **2004**.
[24] a) J. Aizenberg, J. Hanson, T. F. Koetzle, L. Leiserowitz, S. Weiner, L. Addadi, *Chem. Eur. J.* **1995**, *1*, 414 – 422; b) J. Aizenberg, S. Albeck, S. Weiner, L. Addadi, *J. Cryst. Growth* **1994**, *142*, 156 – 164.
[25] a) J. Aizenberg, A. J. Black, G. H. Whitesides, *J. Am. Chem. Soc.* **1999**, *121*, 4500 – 4509; b) D. D. Archibald, S. B. Qadri, B. P. Gaber, *Langmuir* **1996**, *12*, 538 – 546.
[26] A. Berman, D. J. Ahn, A. Lio, M. Salmeron, A. Reichert, D. Charych, *Science* **1995**, *269*, 515 – 518.
[27] J. Lahiri, G. Xu, D. M. Dabbs, N. Yao, I. A. Aksay, J. T. Groves, *J. Am. Chem. Soc.* **1997**, *119*, 5449 – 5450.
[28] The repeat distances of 4.7 and 6.9 Å, which have been observed previously in crystalline β-sheet structures, can be used to estimate the area per molecule. For example, $(4 \times 4.7 \times 6.9)$ Å = 129.7 Å for an eight-residue peptide; see ref. [15].
[29] In aqueous solution the acetylated octapeptide **3** showed a random-coil conformation.
[30] In situ GIXD measurements on water and $CaCl_2$ solution subphases showed that the interstrand distance remained constant upon compression. The strand length, however, appeared to have an elastic behavior, as the conformation of the backbone changed upon compression.
[31] S. Rajam, B. R. Heywood, J. B. A. Walker, S. Mann, R. J. Davey, J. D. Birchall, *J. Chem. Soc. Faraday Trans.* **1991**, *87*, 727 – 734.
[32] a) S. Mann, B. R. Heywood, S. Rajam, J. D. Birchall, *Nature* **1988**, *334*, 692 – 695; b) D. J. Ahn, A. Berman, D. Charych, *J. Phys. Chem.* **1996**, *100*, 12455 – 12461; c) S. J. Cooper, R. B. Sessions, S. D. Lubetkin, *J. Am. Chem. Soc.* **1998**, *120*, 2090 – 2098; d) G. Xu, N. Yao, I. A. Aksay, J. T. Groves, *J. Am. Chem. Soc.* **1998**, *120*, 11977 – 11985.

  